

## The Effect of Laser Annealing on the Surface Morphology and Optical Characteristics of Nanosilicon Films

T.V. Rodionova\*, A.S. Sutyagina†, A.G. Gumenyuk, L.Y. Robur‡

*Taras Shevchenko National University of Kyiv, 64/13, Volodymyrska Str., 01601 Kyiv, Ukraine*

(Received 10 December 2014; published online 25 March 2015)

The effect of laser annealing on the surface microrelief and optical properties of nanocrystalline silicon films, prepared by low pressure chemical vapor deposition, has been investigated. It is shown that under the interaction with the laser radiation recrystallization takes place in the films, due to which there is a smoothing of surface irregularities and forming of grain-agglomerates. These structural changes lead to the decrease in the content of the silicon oxide films by reducing the area of the grain boundaries. The additional peak at 480 nm is observed in the absorption spectrum of the films.

**Keywords:** Nanocrystalline silicon films, Surface roughness, Grain growth, Laser annealing, Optical properties.

PACS numbers: 68.55. – a, 68.60.Wm

### 1. INTRODUCTION

A wide application of silicon films and multilayer structures on their base, in particular, Si film / SiO<sub>2</sub> / monocrystalline Si structures, in microelectronics and solar power engineering necessitates the detailed study of their structure, since just it defines the electrophysical characteristics of elements of integrated-circuits and solar cell as well as their reliability [1-3].

Use of nanomaterials, in particular, nanocrystalline silicon films, is promising from the point of view of application in solar power engineering. Using nanoparticles, it is possible to increase the battery surface area-to-volume ratio, so that the efficiency increases [3]. If, for example, deposit a nanocrystalline silicon film of the thickness to 10 nm on the solar battery surface, its efficiency will increase by 5 %.

Studies focused on improving the structure of these materials are actual to increase the efficiency of nanosilicon materials in their application in solar power engineering. In particular, in order to reduce the solar reflection losses and increase the photoabsorption coefficient of solar radiation by the semiconductor volume, a substantial attention is devoted to the formation of the surface relief of solar cells.

Structure of nanosilicon films and microrelief of their surface are determined by the conditions of the films production and subsequent treatments. A possibility to modify the films structure, their surface and properties of multilayer systems using laser radiation attracts a special attention [4-9]. This is conditioned by the fact that when using laser radiation, there is a possibility of selective annealing of separate layers in multilayer systems by choosing the corresponding wavelength and radiation power that is impossible for ordinary thermal treatments [4, 8].

It is known that depending on the parameters of laser radiation, it is possible to achieve the improvement of quality of the silicon surface on account of recrystal-

lization of polycrystalline or crystallization of amorphous silicon layers. It is shown in the works [5-7] that structure transformation of silicon layers during laser annealing induces the change in their electrophysical and optical properties. We note that use of the system with simultaneous registration of scattered radiation can allow to determine the characteristics of reconstruction of the defect structure [10, 11].

The aim of the present work was the study of the influence of laser annealing on the surface microrelief and optical characteristics of nanocrystalline silicon films in multilayer nanosilicon film / SiO<sub>2</sub> / monocrystalline Si (nano-Si/SiO<sub>2</sub>/Si) systems.

### 2. OBJECT OF STUDY

Films of nanocrystalline silicon were prepared by low-pressure chemical vapor deposition (LPCVD) technique. Plates of monocrystalline silicon with SiO<sub>2</sub> oxide layer of the thickness of ~ 100 nm were used as the substrates. Thickness of silicon films was equal to 10 nm and deposition temperature – 630 °C. Deposited films had a fully crystalline structure at this temperature [12].

Atomic force microscopy method was used for the investigation of the surface microrelief of the films. Images of the films surface were obtained in the scanning atomic force microscope NanoScope IIIa in the trapping mode by silicon probes with the point radius of 10 nm.

Annealing was performed using the single-frequency solid-state pulsed laser with resonator based on Sagnac interferometer: Nd:YAG active medium, radiation wavelength 1.064 μm (linearly polarized radiation), pulse duration 25 ns, pulse energy 30 mJ, pulse repetition rate 1 Hz. Generation at the lowest transverse mode is confirmed by the Gaussian distribution of the radiation intensity in the beam cross-section [13]. Single-frequency generation is checked by the Fabry-Perot interferometer with the base of 22 mm [14]. Annealing time 15 min, energy density 60 mJ/cm<sup>2</sup>.

\* [rodtv@univ.kiev.ua](mailto:rodtv@univ.kiev.ua)

† [nastyasutyagina@gmail.com](mailto:nastyasutyagina@gmail.com)

‡ [robur@univ.kiev.ua](mailto:robur@univ.kiev.ua)

Method based on the modified Beatty method [15] was used to perform the optical measurements. As shown in [16], for three-layer nano-Si/SiO<sub>2</sub>/Si system, reflection coefficient can be written as follows

$$\mathbf{R} = R e^{i\delta} = \frac{r_{01} + \frac{r_{12} + r_{23} e^{-i2\beta_2}}{1 + r_{12} r_{23} e^{-i2\beta_2}} e^{-i2\beta_1}}{1 + r_{01} \frac{r_{12} + r_{23} e^{-i2\beta_2}}{1 + r_{12} r_{23} e^{-i2\beta_2}}} e^{-i2\beta_1}, \quad (1)$$

where  $r_{01}$ ,  $r_{12}$ ,  $r_{23}$  are the amplitude reflection coefficients at the interfaces air/nano-Si, nano-Si/SiO<sub>2</sub>, SiO<sub>2</sub>/Si, respectively;  $\beta$  is the phase thickness:

$$\beta_l = 2\pi \frac{d_l}{\lambda} \sqrt{(n + i\kappa)^2 - \sin^2 \varphi_{in}}, \quad (2)$$

where  $d_l$  is the thickness of the  $l$ -th layer ( $l = 1$  for the nano-Si layer and  $l = 2$  for the SiO<sub>2</sub> layer);  $n$  and  $\kappa$  are the refractive and absorption indexes, respectively;  $\lambda$  is the wavelength of probing radiation;  $\varphi_{in}$  is the incidence angle.

In the interpretation of the ellipsometric data, one has to solve the inverse problem: recovery of the refractive and absorption indices. It is necessary to note that in order to solve the inverse problem on the determination of the refractive and absorption indices of the film, one should solve the transcendent equation (1). To solve it, the numerical analogue of the diagram method was used [17]. At that, as shown in [18], accounting of the phase incursions in the optical wave propagation in non-uniform absorbing medium allows to describe more precisely the scattering processes, and, so, to obtain a more exact solution of the inverse problem.

The relative measurement error of the absorption coefficient  $\alpha$ :

$$\alpha_{\text{nano-Si}} = \frac{2\pi}{\lambda} \kappa_{\text{nano-Si}}, \quad (3)$$

(which is determined by the accuracy of reading of the incidence angle, polarizer and analyzer azimuths and estimated from successive measurements of the photovoltage) did not exceed the value of 3 %.

Measurement of the spectral dependences was carried out on air at room temperature.

### 3. RESULTS AND DISCUSSION

AFM-images of the surface of nanocrystalline silicon film before and after laser annealing are represented in Fig. 1. As seen, surface morphology after annealing is significantly changed. In particular, both the sizes of the surface irregularities (height) and their horizontal sizes (grains sizes) are changed. Thus, if sizes of the surface irregularities before annealing were varied in the range of 0÷9 nm (Fig. 1a), then after annealing surface becomes more smooth, sizes of the surface irregularities are changed in the range of 0÷2 nm (Fig. 1b).

In Fig. 2 we illustrate the distributions of the grain sizes for nanosilicon films before and after annealing.

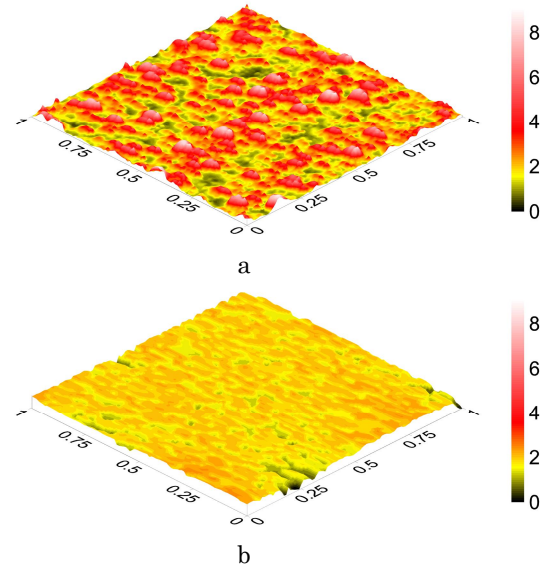


**Fig. 1** – AFM-images of the nanosilicon film surface before (a) and after (b) laser annealing. Lateral sizes are given in microns, height – in nanometers

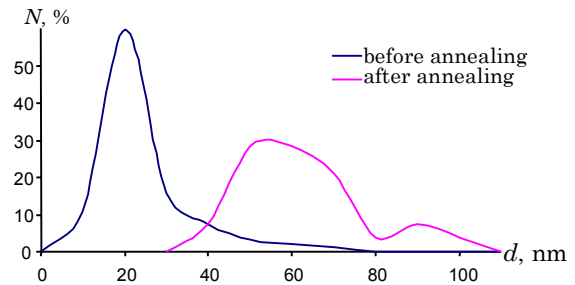


**Fig. 2** – Distribution of the grain sizes in the nanosilicon films before and after laser annealing

As seen, grain sizes before annealing are changed in a narrow range and their mean size is equal to 20 nm. After annealing grains are combined into agglomerates (Fig. 1b) the sizes of which are changed in a wide range (Fig. 2). It is known [4-8, 19] that recrystallization of silicon films takes place under the action of laser irradiation. In this case, three main growth regimes of crystals can be realized: the regime of partial, almost complete and complete melting. Analysis of the AFM-images of the surface of nanosilicon films (shape and sizes of grains-agglomerates) allows to suggest that melting of silicon films occurs during laser annealing.

Since nano-Si films are isotropic, it is possible to assume that they will not differ substantially (from the point of view of polarization characteristics) from a bulk sample. As seen from the angular dependences (Fig. 3), behavior of the dependences is similar, they only have another values of  $R_p$  and  $R_s$  and shifted position of the chief angle (the values of the chief angle are  $\sim 51^\circ$  for the SiO<sub>2</sub>/Si system, while for the nano-Si/SiO<sub>2</sub>/Si they are changed from  $\sim 57^\circ$  to  $\sim 54^\circ$ ).

In Table 1 we present the data of the structures determined by the angular dependences of the ellipsometric parameters.

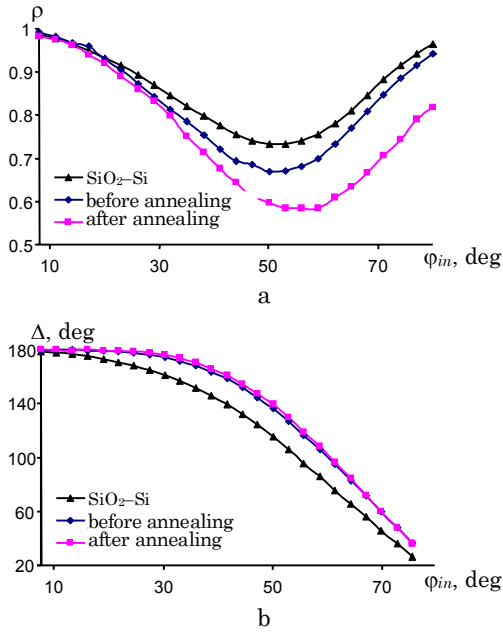


**Fig. 3** – Angular dependences of the ellipsometric parameters ( $\rho = R_p/R_s$  and  $\Delta = \delta_{RP} - \delta_{RS}$ ) for the nano-Si-SiO<sub>2</sub>-Si system in comparison with the SiO<sub>2</sub>-Si system [4]

**Table 1** – Values of the characteristics of different structures determined by the angular dependences ( $\lambda = 633$  nm)

Structure		nano-Si	SiO <sub>2</sub>	Si
SiO <sub>2</sub> -Si	$n$		1.54	4.05
	$\kappa$		0.013	0.027
	$d$ , nm		101	
nano-Si-SiO <sub>2</sub> -Si before annealing	$n$	3.28	1.51	4.04
	$\kappa$	0.017	0.011	0.027
	$d$ , nm	11	104	
nano-Si-SiO <sub>2</sub> -Si after annealing	$n$	3.57	1.51	4.04
	$\kappa$	0.021	0.012	0.027
	$d$ , nm	10	103	

It is seen that annealing of the nano-Si film leads to the increase in the refractive ( $n$ ) and absorption ( $\kappa$ ) indices. At that, since films of nanocrystalline silicon can be considered as nanosized crystallites surrounded by the oxide layers [20], then applying the effective medium model [21] one can determine the percentage contribution of the components.

Estimations of the content of the components were performed by two models: the Maxwell-Garnett [22] and Bruggeman [23]. According to the Maxwell-Garnett model which is true in the case when one of the components is a point inclusion into another, the effective complex refractive index is calculated as follows:

$$\frac{N_{\text{nano-Si}}^2 - N_{\text{SiO}_2}^2}{N_{\text{nano-Si}}^2 + 2N_{\text{SiO}_2}^2} = f_{\text{Si}} \frac{N_{\text{Si}}^2 - N_{\text{SiO}_2}^2}{N_{\text{Si}}^2 + 2N_{\text{SiO}_2}^2}, \quad (4)$$

where  $N = n + i\kappa$  is the complex refractive index;  $f$  is the volumetric filling factor (concentration). The estimated value of the volumetric concentration of silicon oxide is 32.1 % before annealing and 19.9 % – after annealing. We note that validity of the Maxwell-Garnett model can be violated at  $f > 10$  % [21].

Therefore, in order to estimate the percentage of the oxide, we have used the Bruggeman model, where the

volumetric filling factor is determined from the following system [23]

$$\begin{cases} f_{\text{SiO}_2} \frac{N_{\text{SiO}_2}^2 - N_{\text{nano-Si}}^2}{N_{\text{SiO}_2}^2 + 2N_{\text{nano-Si}}^2} + f_{\text{Si}} \frac{N_{\text{Si}}^2 - N_{\text{nano-Si}}^2}{N_{\text{Si}}^2 + 2N_{\text{nano-Si}}^2} = 0, \\ f_{\text{SiO}_2} + f_{\text{Si}} = 1. \end{cases} \quad (5)$$

The estimated value of the volume concentration of silicon oxide in the Bruggeman model is equal to 29.4 % before annealing and 18.7 % – after annealing. Such a decrease in the silicon oxide content in the films after laser annealing is associated with the change in the nanosilicon film structure. In particular, the number and area of the boundaries in the film decrease during the formation of grains-agglomerates. Since impurities, in particular, oxygen, segregate at the grain boundaries, then decrease in the number of boundaries leads to the reduction of the oxygen content and, correspondingly, to the silicon oxide content in the films.

Recovered spectral dependences of the film absorption coefficient before and after laser annealing compared with absorption coefficients of Si are represented in Fig. 4.

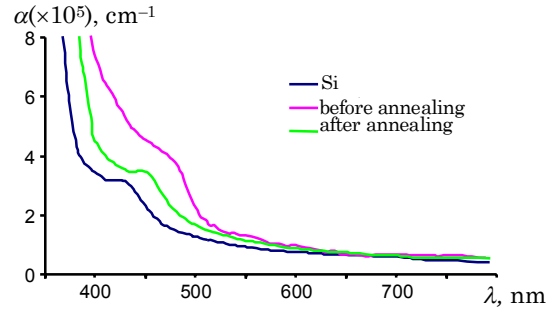


**Fig. 4** – Spectral dependences of the absorption coefficient ( $\alpha$ ) for the nano-Si film in comparison with Si

It is necessary to note that a quasi-periodic structure, which can appear due to the scattering on separate film clusters, is absent on the spectral dependences [16]. At that, laser treatment leads to the shift of the absorption edge of the nano-Si film towards smaller wavelengths approximately by 20 nm. As seen, an additional band with the maximum at 480 nm (for pure silicon maximum is at 440 nm) appears in the absorption spectrum of the nano-Si film. The same effect of the laser treatment influence was observed for the transmission spectra of the quartz/Si, quartz/Si/SiO<sub>2</sub> and SiC/Si/SiO<sub>2</sub> structures [20]. Shift of the absorption edge observed in the spectra of nano-Si correlates with the data of [21], where it is shown that influence of a powerful laser radiation on thin Si films on the SiO<sub>2</sub> surface leads to the same effect on account of silicon recrystallization.

#### 4. CONCLUSIONS

1. Experimental investigations have shown that laser annealing of nanocrystalline silicon films in multilayer nano-Si/SiO<sub>2</sub>/Si systems leads to the substantial decrease in the sizes of surface irregularities and formation of the grains-agglomerates, whose sizes several times exceed the initial grain sizes in the films before annealing.

2. Using the angular dependences of the ellipsometric parameters it is established that silicon oxide content in

the films decreases after annealing due to the decrease in the area of grain boundaries during grain growth.

3. Laser annealing leads to the shift of the absorption

edge of nanosilicon films towards smaller wavelengths. Maximum in the vicinity of 480 nm appears in the absorption spectrum.

## REFERENCES

1. S. Mukhopadhyay, A. Chowdhury, *Thin Solid Films* **516**, 6824 (2008).
2. J.K. Rath, *Sol. Energ. Mater. Sol. C.* **76**, 431 (2003).
3. V.V. Sychov, *Ros. khim. zh. (Zh. Ros. khim. Ob-va im. D.I. Mendeleeva)* **LII** No 6, 118 (2008).
4. O.M. Zhigalina, D.N. Khmelenin, K.A. Vorotilov, A.S. Sigov, I.G. Lebo, *Solid State Phys.* **51** No 7, 1482 (2009).
5. T. Sameshima, H. Watakabe, N. Andoh, S. Higashi, *Jpn. J. Appl. Phys.* **45**, 2437 (2006).
6. M. Modreanu, M. Gartner, C. Cobianu, B. O'Looney, F. Murphy, *Thin Solid Films* **450**, 105 (2004).
7. Ye.Yu. Volkov, V.N. Lisochenko, R.V. Konakova, O.B. Okhrimenko, A.M. Svetlichnyi, *Izvestiya vysshikh uchebnykh zavedeniy. Fizika.* 143, (2011).
8. V.N. Lissotschenko, R.V. Konakova, B.G. Konoplev, V.V. Kushnir, O.B. Okhrimenko, A.M. Svetlichnyi, *Semiconductors* **44** No 3, 326 (2010).
9. V.A. Karachinov, *Semiconductors* **31** No 1, 44 (1997).
10. O.I. Barchuk, A.A. Goloborodko, V.N. Kurashov, Y.A. Oberemok, S.N. Savenkov, *Proc. of SPIE* **6254**, 62540W (2006).
11. A.A. Goloborodko, *Proc. of SPIE* **9066**, 90660Z (2013).
12. N.G. Nakhodkin, T.V. Rodionova, *phys. status solidi a* **123**, 431 (1991).
13. M.U. Bilyi, I.V. Zakharchenko, V.P. Koshelenko, B.A. Okhrimenko, *Ukr. J. Phys.* **46**, 1133 (2001).
14. I.V. Zakharchenko, O.V. Krylov, S.H. Nedil'ko, L.Y. Robur, *Visnyk Kyyivs'koho natsional'noho universytetu imeni Tarasa Shevchenka. Seriya fizyka* **12**, 15 (2011).
15. J.R. Beattie, G.K.T. Conn, *Philosophical Magazine* **43**, 222 (1955).
16. A.A. Goloborodko, M.V. Eпов, L.Y. Robur, T.V. Rodionova, *J. Nano- Electron. Phys.* **6** No 2, 02002 (2014).
17. R.J. Archer, *J. Opt. Soc. Am.* **52**, 970 (1962).
18. A.A. Goloborodko, *J. Nano- Electron. Phys.* **5** No 3, 03048 (2013).
19. Zhijun Yuan, Qihong Lou, Jun Zhou, Jingxing Dong, Yunrong Wei, Zhijiang Wang, Hongming Zhao, Guohua Wu, *Opt. Laser Technol.* **41**, 380 (2009).
20. P.G. Sennikov, S.V. Golubev, V.I. Shashkin, D.A. Pryakhin, M.N. Drozdov, B.A. Andreev, Yu.N. Drozdov, A.S. Kuznetsov, H.-J. Pohl, *Semiconductors* **43** No 7, 968 (2009).
21. L.A. Golovan, V.Yu. Timoshenko, P.K. Kashkarov, *Phys. Usp.* **50**, 595 (2007).
22. J.C. Maxwell-Garnett, *Philos. Trans. R. Soc. London A* **203**, 385 (1904).
23. D.A.G. Bruggeman, *Ann. Phys.* **24**, 636 (1935).